Synthesis of Oppositely Charged Block Copolymers of Poly(ethylene glycol) via Reversible Addition−Fragmentation Chain Transfer Radical Polymerization and Characterization of Their Polyion Complex Micelles in Water

Shin-ichi Yusa,*,† Yuuichi Yokoyama,† and Yotaro Morishima‡

Department of Materials Science and Chemistry, Graduate School of Engineering, University of Hyogo, 2167 Shosha, Himeji, Hyogo 671-2280, Japan and Faculty of Engineering, Fukui University of Technology, 6-3-1 Gakuen, Fukui 910-8505, Japan

Received September 17, 2008; Revised Manuscript Received November 18, 2008

ABSTRACT: Diblock copolymers consisting of a water-soluble nonionic block and either an anionic or cationic block were prepared from sodium 2-(acrylamido)-2-methylpropanesulfonate (AMPS) or (3-(methacryloylamino)propyl)trimethylammonium chloride (MAPTAC) via reversible addition−fragmentation chain transfer (RAFT)-controlled radical polymerization using poly(ethylene glycol) (PEG)-based chain transfer agent (PEG-CTA) in water. The RAFT polymerization proceeded in a living fashion, as suggested by the observation that the number-average molecular weight (M_n) increased linearly with the monomer conversion (up to conversions of 30% for MAPTAC and 50% for AMPS), whereas the polydispersity (M_w/M_n) remained nearly constant ($M_w/M_n < 1.05$ for MAPTAC and <1.2 for AMPS) independent of the conversion. The mixing of aqueous solutions of the oppositely charged diblock copolymers, PEG-*b*-PAMPS and PEG-*b*-PMAPTAC, led to the spontaneous formation of polyion complex (PIC) micelles. The PIC micelles were characterized by ^{1}H NMR spin−spin relaxation time, static light scattering (SLS), dynamic light scattering (DLS), and scanning electron microscopy (SEM) techniques. The hydrodynamic size of the micelle depended on the mixing ratio of PEG-*b*-PAMPS and PEG-*b*-PMAPTAC with the size maximizing at the mixing ratio of stoichiometric charge neutralization. The mixing of the oppositely charged diblock copolymers with shorter charged blocks formed a core−shell PIC micelle. In contrast, a complicated aggregate was formed from a pair of longer blocks. The exact structure of the aggregate is still an open question, but it is speculated to be a multicore intermicellar aggregate on the basis of various characterization data.

Introduction

Self-association of block copolymers in solution has been widely used to prepare polymer-based nanostructured materials such as micelles (spherical or cylindrical) and vesicles.[1] Generally, the self-association is driven by noncovalent interactions including hydrogen bonding, van der Waals, hydrophobic, and electrostatic interactions. Increasing attention has been given to the hydrophobically driven self-association of amphiphilic diblock copolymers because polymer micelles with a core−shell structure thus formed have been thought to be potentially important in many applications including separation[2] and delivery systems.[3]

A great deal of effort has been devoted to the investigation of polyion complex (PIC) micelles.[4−7] A pair of oppositely charged block copolymers consisting of a poly(ethylene glycol) (PEG) block and a charged block forms water-soluble PIC micelles composed of a PEG shell and segregated PIC core. Kataoka and Harada were the first to report on this type of PIC micelle prepared from a pair of oppositely charged poly(amino acid) block copolymers of PEG.[8−10] The authors have demonstrated that PIC micelles formed from a mixture of poly(ethylene glycol)-*block*-poly(L-lysine) (PEG-P(Lys)) and poly(ethylene glycol)-*block*-poly(α,β-asparatic acid) (PEG-P(Asp)) are monodisperse. Matched pairs with the same block length of polyanions and polycations formed core−shell type assemblies with extremely narrow size distribution.[11]

The recent development of living free radical polymerization methods have provided a useful tool for the syntheses of various block copolymers with a controlled structure, allowing one to utilize a wide variety of monomers that can undergo polymerization with only a free-radical mechanism. Among living radical polymerization techniques, the reversible addition−fragmentation chain transfer (RAFT) radical polymerization method offers advantages because it is a metal-free method that uses only a dithioester group containing chain transfer agent (CTA) added to a conventional free radical polymerization medium. Thus, water-soluble charged vinyl polymers and their block copolymers can be easily prepared via RAFT-controlled radical polymerization.[12−14] The versatility and usefulness of the RAFT technique have been comprehensively discussed in excellent review articles authored recently by McCormick and Lowe.[15,16]

In this article, we report on the synthesis of oppositely charged diblock copolymers made up of a nonionic PEG block and a charged block (Scheme 1), that is, poly(ethylene glycol)-*block*-poly((3-(methacryloylamino)propyl)trimethylammonium chloride) (PEG-*b*-PMAPTAC) and poly(ethylene glycol)-*block*-poly(sodium 2-(acrylamido)-2-methylpropanesulfonate) (PEG-*b*-PAMPS) by RAFT polymerization using PEG-based CTA. These diblock copolymers assemble in a PIC micelle when mixed together in water. We also report herein on the characterization of PIC micelles formed from PEG-*b*-PMAPTAC and PEG-*b*-PAMPS with different charged block lengths in water.

Experimental Section

Materials. 4-Cyanopentanoic acid dithiobenzoate (CPD) was synthesized according to the method reported by McCormick and coworkers.[17] Dichloromethane was dried over 4 Å molecular sieves and was distilled. Poly(ethylene glycol) methyl ether (MeOPEG; average molecular weight, ∼2000) from Aldrich was used as received without further purification. (3-(Methacryloylamino)pro-

* To whom correspondence should be addressed. E-mail: yusa@eng.u-hyogo.ac.jp.
† University of Hyogo.
‡ Fukui University of Technology.

10.1021/ma8021162 CCC: $40.75
Published on Web 12/18/2008

Scheme 1

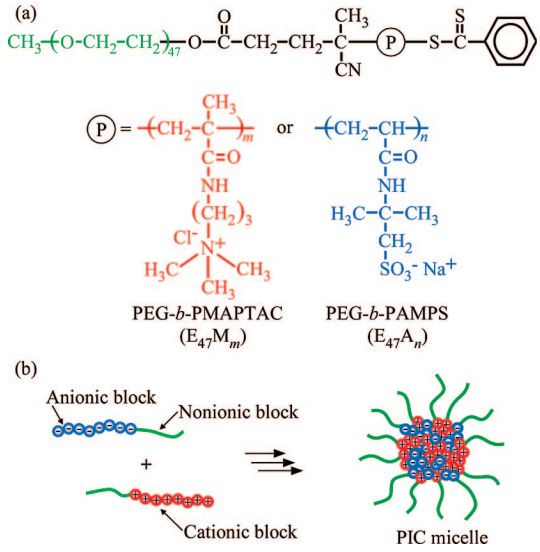

(a) Chemical structures of diblock copolymers, PEG-*b*-PMAPTAC ($E_{47}M_m$) and PEG-*b*-PAMPS ($E_{47}A_n$), used in this study. (b) Schematic representation of a polyion complex (PIC) micelle composed of $E_{47}M_m$ and $E_{47}A_n$.

pyl)trimethylammonium chloride (MAPTAC) (50 wt % in water) from Aldrich was passed through an inhibitor-remover column. 2-(Acrylamido)-2-methylpropanesulfonic acid (AMPS) (95%) and 4,4′-azobis(4-cyanopentanoic acid) (V-501) (98%) from Wako Pure Chemical were used as received without further purification. Water was purified with a Millipore Milli-Q system. Other reagents were used as received.

Synthesis of Poly(ethylene glycol)-Based Chain Transfer Agent (PEG-CTA). PEG-CTA was synthesized according to the literature with slight modification.[18] A CH_2Cl_2 solution (100 mL) of *N*,*N*′-dicyclohexylcarbodiimide (DCC) (5.66 g, 27.4 mmol) was added dropwise to a CH_2Cl_2 solution (100 mL) of MeOPEG (27.4 g, 13.0 mmol), CPD (4.60 g, 16.5 mmol), and a trace of 4-(dimethylamino)pyridine over a period of 30 min. After the reaction mixture was stirred for 20 h at 40 °C, it was filtrated to remove dicyclohexylurea. The solvent was removed, and the crude product was purified on a silica gel column using a mixture of $CHCl_3$ and methanol (95/5 v/v) as eluent, affording 14.0 g of PEG-CTA as a red powder (44.8% yield). ^{1}H NMR ($CDCl_3$, δ): 2.17 (s, 3H), 2.40−2.74 (m, 4H), 3.38 (s, 3H), 3.45−4.25 (m, 188H), 4.27 (t, 2H), 7.40 (t, 2H), 7.57 (t, 1H), 7.90 (d, 2H).

Preparation of Cationic Diblock Copolymer (PEG-*b*-PMAPTAC). A representative example for the preparation of the diblock copolymer of PEG and PMAPTAC is as follows: MAPTAC (5.96 g, 27.0 mmol), V-501 (35.0 mg, 0.123 mmol), and PEG-CTA (565 mg, 0.250 mmol) were dissolved in water (30.3 mL). The mixture was degassed by purging with Ar gas for 30 min. Polymerization was carried out at 70 °C for 5 h. The polymerization mixture was poured in a large excess of acetone to precipitate the resulting polymer. The polymer was purified by reprecipitating from methanol in an excess of acetone twice. The cationic diblock copolymer obtained was dried in a vacuum oven at 60 °C for 24 h (6.03 g, 98.9%). The number-average molecular weight (M_n) and the ratio of the weight-average molecular weight to M_n (M_w/M_n), a polydispersity index (PDI), were estimated by gel permeation chromatography (GPC) to be 1.51×10^4 and 1.02, respectively. The number-average degree of polymerization (DP_n) for the PMAPTAC block was 106, as estimated by ^{1}H NMR.

Preparation of Anionic Diblock Copolymer (PEG-*b*-PAMPS). A representative example for the preparation of the diblock copolymer of PEG and PAMPS is as follows: A predetermined amount of AMPS (5.60 g, 27.0 mmol) was neutralized with NaOH (1.08 g, 27.0 mmol) in 30.6 mL of water. To this solution was added predetermined amounts of V-501 (35.0 mg, 0.123 mmol) and PEG-CTA (566 mg, 0.251 mmol). The solution was degassed by purging with Ar gas for 30 min. Polymerization was carried out at 70 °C for 5 h. The polymerization mixture was poured in a large excess of ethanol to precipitate the resulting polymer. The polymer was purified by reprecipitating from water in an excess of ethanol twice. The anionic diblock copolymer obtained was dried in a vacuum oven at 60 °C for 24 h (5.84 g, 92.4%). The M_n and M_w/M_n values determined by GPC were 2.30×10^4 and 1.17, respectively. DP_n for the PAMPS block was 108, as estimated by ^{1}H NMR.

Polymerization of MAPTAC in D_2O. Predetermined amounts of MAPTAC (1.10 g, 5.00 mmol), PEG-CTA (0.113 g, 0.05 mmol), and V-501 (6.90 mg, 0.025 mmol) were dissolved in 6.04 mL of D_2O. The solution was transferred to several NMR tubes and degassed by purging with Ar gas for 30 min. The cap was sealed, and the solution was heated to 70 °C in a preheated oil bath for varying lengths of reaction time. Polymerization was terminated by rapid cooling in an ice bath. The monomer conversion estimated from ^{1}H NMR was monitored as a function of reaction time. GPC for the reaction mixture was measured to estimate M_n and M_w/M_n. Polymerization of AMPS using PEG-CTA in D_2O was carried out in a similar manner.

Measurements. *Gel Permeation Chromatography.* GPC measurements for cationic polymer samples were performed using a refractive index (RI) detector equipped with a Shodex 10 μm bead size Ohpak SB-804 HQ column (exclusion limit ~10^7) working at 40 °C under a flow rate of 0.6 mL/min. A 0.3 M Na_2SO_4 aqueous solution containing 0.5 M acetic acid was used as eluent. The values of M_n and M_w/M_n for cationic polymer samples were calibrated with standard poly(2-vyniypyridine) samples of six different molecular weights ranging from 5.70×10^3 to 3.16×10^5. GPC measurements for anionic polymer samples were performed using an RI detector equipped with a Shodex 7.0 μm bead size GF-7 M HQ column (exclusion limit ~10^7) working at 40 °C under a flow rate of 0.6 mL/min. A phosphate buffer (pH 9) containing 10 vol % acetonitrile was used as eluent. The values of M_n and M_w/M_n for anionic polymers were calibrated with standard sodium polystyrene sulfonate samples of 11 different molecular weights ranging from 1.37×10^3 to 2.16×10^6.

Proton Nuclear Magnetic Resonance. ^{1}H NMR spectra were obtained with a Bruker DRX-500 spectrometer operating at 500 MHz using deuterium lock at a constant temperature of 20 °C during the whole run. The sample solutions of the polymer for ^{1}H NMR measurements were prepared in D_2O containing 0.1 M NaCl. The polymer concentration (C_p) was 1.0 g/L. ^{1}H NMR spin−spin relaxation time (T_2) was determined by the Carr−Purcell−Meiboom−Gill (CPMG) method.[19,20] For T_2 measurements, NMR tubes containing D_2O solution were deaerated by purging with Ar gas for 30 min. A 90° pulse of 13.85 μs was calibrated and used for the measurement. Echo peak intensities at 12 different numbers of the 180° pulse were measured.

Light Scattering Measurements. Light scattering measurements were performed using an Otsuka Electronics Photal DLS-7000HL light scattering spectrometer equipped with a multi-τ digital time correlator (ALV-5000E). A He−Ne laser (10.0 mW at 632.8 nm) was used as a light source. Sample solutions for light scattering measurements were filtered by a 0.2 μm pore size membrane filter.

In static light scattering (SLS) measurements, the weight-average molecular weight (M_w), z-average radius of gyration (R_g), and second virial coefficient (A_2) values were estimated from the relation

$$\frac{KC_p}{R_\theta} = \frac{1}{M_w}\left(1 + \frac{1}{3}R_g^2 q^2\right) + 2A_2C_p \qquad (1)$$

where R_θ is the difference between the Rayleigh ratio of the solution and that of the solvent, $K = 4\pi^2 n^2 (dn/dC_p)^2/N_A\lambda^4$ with dn/dC_p being the RI increment against C_p and with N_A being Avogadro's number and q being the magnitude of scattering vector. The q value is calculated from $q = (4\pi n/\lambda)(\sin(\theta/2))$, where n is the RI of the solvent, λ is the wavelength of light source (= 632.8 nm), and θ is

scattering angle. By measuring R_θ for a set of C_p and θ, values of M_w, R_g, and A_2 were estimated from Zimm plots. The known Rayleigh ratio of toluene was used for the calibration of the instrument. Values of dn/dC_p at 633 nm were determined with an Otsuka Electronics Photal DRM-3000 differential refractometer.

In dynamic light scattering (DLS) measurements, to obtain the relaxation time distribution, $\tau A(\tau)$, the inverse Laplace transform (ILT) analysis was performed using the algorithm REPES[21−23]

$$g^{(1)}(t) = \int \tau A(\tau) \exp(-t/\tau)\, d \ln \tau \quad (2)$$

where τ is the relaxation time and $g^{(1)}(t)$ is the normalized autocorrelation function. The relaxation rate ($\Gamma = \tau^{-1}$) is a function of C_p and θ.[24] The diffusion coefficient in the limit of zero angle (D) was calculated from $D = (\Gamma/q^2)_{q\to 0}$. The infinite dilution diffusion coefficient (D_0) was calculated from

$$D_0 = D/(1 + k_d C_p) \quad (3)$$

where k_d is the hydrodynamic virial coefficient. The hydrodynamic radius (R_h) is given by the Stokes−Einstein equation, $R_h = k_B T/(6\pi\eta D_0)$, where k_B is the Boltzmann constant, T is the absolute temperature, and η is the solvent viscosity. The details of DLS instrumentation and theory are described in the literature.[25−27]

Scanning Electron Microscopy. SEM analyses were carried out on a JEOL JSM-5310 apparatus with an accelerating voltage of 10 kV. A sample for SEM observation was prepared by dropping a sample solution on a clean glass slide followed by completely drying at room temperature. The specimen thus prepared was coated with Pt using a JEOL JFC-1600 sputter coating instrument.

Preparation of Polyion Complex Micelles. PEG-*b*-PMAPTAC and PEG-*b*-PAMPS were separately dissolved in an aqueous solution containing 0.1 M of NaCl, and the solutions were allowed to stand overnight at room temperature to achieve complete dissolution. For the preparation of PIC micelles, a PEG-*b*-PMAPTAC solution was added dropwise to a PEG-*b*-PAMPS solution over a period of 5 min at room temperature with stirring, and the mixture was allowed to equilibrate for at least 1 day prior to measurement. The mixing ratio of the two block copolymers in solution was represented by the mole fraction of positively charged unit ($f^+ = [\text{MAPTAC}]/([\text{AMPS}] + [\text{MAPTAC}])$), and hence the complete charge neutralization is attained at $f^+ = 0.5$. The PIC micelles were prepared at $f^+ = 0.5$ unless otherwise noted.

Results and Discussion

Synthesis of Diblock Copolymers. To prepare diblock copolymers consisting of nonionic PEG and ionic blocks, we performed RAFT radical polymerization of ionic monomers using PEG-CTA. PEG-CTA was synthesized via the esterification of the terminal hydroxyl group of MeOPEG with CPD.[28,29] The RAFT polymerization of MAPTAC by the use of PEG-CTA proceeded in a controlled manner as illustrated in Figure 1. In Figure 1a, a time-conversion relationship is depicted along with the first-order kinetics plot for the polymerization of MAPTAC in the presence of PEG-CTA ($M_n = 2.38 \times 10^3$ estimated from ^{1}H NMR) at 70 °C in D_2O under an Ar atmosphere. The monomer consumption was monitored by ^{1}H NMR spectroscopy as a function of polymerization time. There is an induction period of ca. 31 min, which may be due to a slow rate of the formation of the 4-cyanopentanoic acid radical fragment, as reported by McCormick and coworker.[30] A monomer conversion of 89.5% was reached within 180 min. The kinetics plot for the RAFT polymerization of MAPTAC shown in Figure 1a indicates that the concentration of active species remains constant during the polymerization.

Figure 1b shows GPC elution curves (RI response) for the polymerization of MAPTAC in the presence of PEG-CTA. A significant increase in the molecular weight occurs upon polymerization of MAPTAC, indicating the formation of the

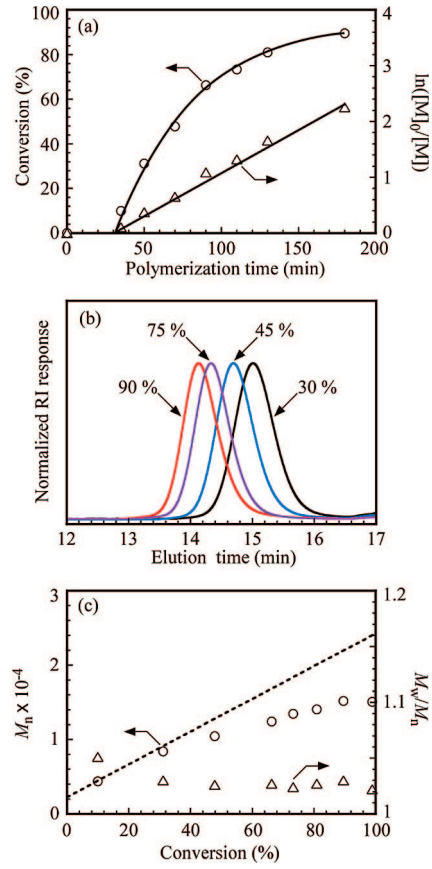

Figure 1. (a) Time-conversion (○) and the first-order kinetics plots (Δ) for the polymerization of MAPTAC in the presence of PEG-CTA in D_2O at 70 °C. (b) GPC elution curves demonstrating the evolution of molecular weight during the synthesis of PEG-*b*-PMAPTAC using PEG-CTA. Conversions are shown for each peak. (c) Dependence of M_n (○) and M_w/M_n (Δ) on the monomer conversion in the polymerization of MAPTAC in the presence of PEG-CTA. The dotted line represents the theoretical results.

block copolymer, PEG-*b*-PMAPTAC. Neither a new peak nor a shoulder due to homopolymers of MAPTAC was recognized. Thus, it was concluded that no homopolymerization of MAPTAC occurred concurrently. In Figure 1c, values of M_n and M_w/M_n estimated from GPC for the diblock copolymers are plotted as a function of the conversion of MAPTAC determined by ^{1}H NMR. The M_n value increases with conversion, whereas M_w/M_n remains fairly constant ($M_w/M_n < 1.05$) independent of the conversion. If the polymerization is assumed to be ideally living in nature, then the theoretical number-average molecular weight (M_n(theor)) can be calculated to be

$$M_n(\text{theor}) = \frac{[\text{monomer}]_0}{[\text{PEG}-\text{CTA}]_0}\frac{x_m}{100}M_m + M_{\text{PEG-CTA}} \quad (4)$$

where $[\text{monomer}]_0$ is the initial monomer concentration, $[\text{PEG-CTA}]_0$ is the initial PEG-CTA concentration, x_m is the percent conversion of monomer, M_m is the molecular weight of monomer, and $M_{\text{PEG-CTA}}$ is the molecular weight of PEG-CTA. A theoretical line calculated from eq 4 is depicted in Figure 1c. Observed values of M_n agree reasonably well with theoretical values in a low M_n region, but the M_n plots deviate considerably from the theoretical line when $M_n > 1 \times 10^4$. At present, the reason for the considerable deviation is an open question, but it may be due to the use of poly(2-vynilpyridine) as a standard polymer to calibrate M_n values, of which the volume-to-mass ratio may be very different from that of PEG-*b*-PMAPTAC.[31,32] Number-average molecular weights (M_n(NMR)) for PEG-*b*-

Table 1. Number-Average Molecular Weight (M_n), Molecular Weight Distribution (M_w/M_n), and Hydrodynamic Radius (R_h) of the Block Copolymers Used in This Study

samples		M_n(theor) × 10^{-4a}	M_n(GPC) × 10^{-4b}	M_n(NMR) × 10^{-4c}	M_w/M_n(GPC)^b	R_h (nm)^d
PEG-*b*-PMAPTAC	$E_{47}M_{27}$	0.78	0.82	0.83	1.03	4.5
	$E_{47}M_{106}$	2.52	1.51	2.58	1.02	5.1
PEG-*b*-PAMPS	$E_{47}A_{29}$	0.80	0.67	0.90	1.15	5.6
	$E_{47}A_{108}$	2.63	2.30	2.71	1.17	6.1

[a] Calculated from eq 4. [b] Estimated from GPC. [c] Estimated from ^{1}H NMR for the purified diblock copolymers. [d] Determined by DLS at 20 °C in 0.1 M NaCl aqueous solution at C_p = 1.0 g/L.

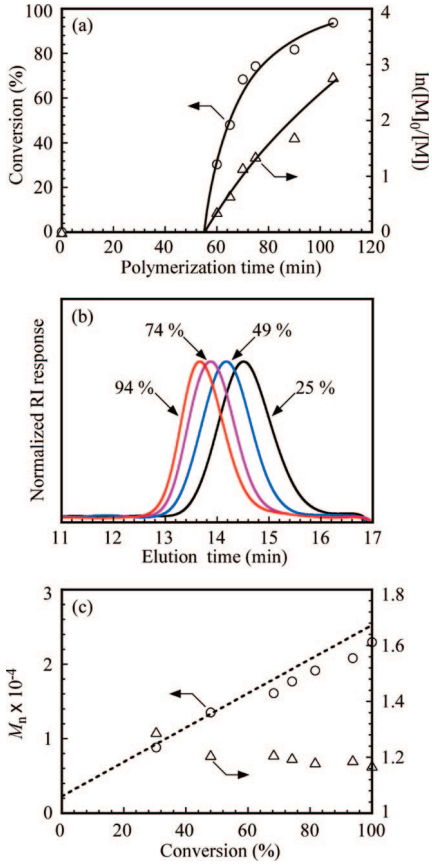

Figure 2. (a) Time-conversion (○) and the first-order kinetics plots (Δ) for the polymerization of AMPS in the presence of PEG-CTA in D_2O at 70 °C. (b) GPC elution curves demonstrating the evolution of the molecular weight during the synthesis of PEG-*b*-PAMPS using PEG-CTA. The monomer conversion is indicated for each elution curve. (c) Dependence of M_n (○) and M_w/M_n (Δ) on the monomer conversion in the polymerization of AMPS in the presence of PEG-CTA. The dotted line represents the theoretical results.

PMAPTAC samples were calculated from ^{1}H NMR data. As compared in Table 1, M_n(NMR) values for PEG-*b*-PMAPTAC are in fair agreement with M_n(theor) values.

The polymerization of AMPS in the presence of PEG-CTA also proceeded in a controlled manner, as illustrated in Figure 2. In Figure 2a are shown time-conversion and first-order kinetics plots. The polymerization started after an induction period of ca. 55 min and reached a monomer conversion of 93.8% within 105 min. As can be seen from GPC elution curves shown in Figure 2b, the molecular weight of the resulting block polymer, PEG-*b*-PAMPS, increases with the monomer conversion, and the molecular weight distribution is unimodal. Values of M_n and M_w/M_n estimated from GPC are plotted in Figure 2c as a function of the conversion. The M_n value increases almost linearly with the conversion up to ~50% conversion, whereas M_w/M_n lies in a somewhat narrow range of 1.17 to 1.29 independent of the conversion. Compared with the case of PEG-*b*-PMAPTAC, values of M_n estimated by GPC are relatively close to the theoretical values calculated from eq 4.

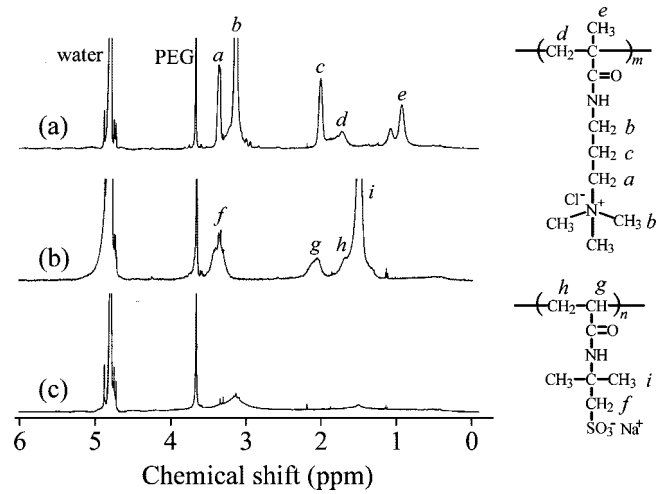

Figure 3. ^{1}H NMR spectra measured at C_p = 1.0 g/L in D_2O containing 0.1 M NaCl for (a) PEG-*b*-PMAPTAC ($E_{47}M_{106}$), (b) PEG-*b*-PAMPS ($E_{47}A_{108}$), and (c) the PIC micelle formed from $E_{47}M_{106}/E_{47}A_{108}$ with f^+ = 0.5. Assignments are indicated for the resonance peaks.

In this work, we prepared a set of PEG-*b*-PMAPTAC and PEG-*b*-PAMPS samples with different lengths of charged blocks, whereas the length of the PEG blocks were the same (M_n(NMR) = 2.38 × 10^3, DP_n = 47). Values of M_n and M_w/M_n for all of the block copolymers are listed in Table 1. The block copolymers, PEG-*b*-PMAPTAC and PEG-*b*-PAMPS, are further abbreviated as $E_{47}M_m$ and $E_{47}A_n$; E, M, and A represent PEG, PMAPTAC, and PAMPS blocks of DP_n = 47, *m*, and *n*, respectively.

Proton Nuclear Magnetic Resonance. ^{1}H NMR spectra for PEG-*b*-PMAPTAC ($E_{47}M_{106}$) and PEG-*b*-PAMPS ($E_{47}A_{108}$) are illustrated in Figure 3a,b, respectively. As shown in Figure 3a, the resonance bands observed in the region of 0.8 to 1.1 ppm and at 1.8 ppm are attributed to the α-methyl protons and main chain methylene protons, respectively. DP_n (= *m*) and M_n(NMR) of the PMAPTAC block in $E_{47}M_m$ were determined from the intensity ratio of the resonance bands due to the methyl and methylene protons in the side chain of the PMAPTAC block around 2.9 to 3.4 ppm and the PEG main chain protons at 3.7 ppm. As given in Figure 3b, resonance bands observed at 1.2 to 2.4 ppm for $E_{47}A_n$ are attributed to the sum of the main chain and pendent methyl groups in the PAMPS block. DP_n (= *n*) and M_n(NMR) of the PAMPS block in $E_{47}A_n$ were calculated from the intensity ratio of the resonance bands due to the pendent methylene protons of the PAMPS block at 3.4 ppm and PEG main chain protons at 3.7 ppm.

Figure 3c shows a ^{1}H NMR spectrum for a mixed solution of $E_{47}M_{106}$ and $E_{47}A_{108}$ with 0.5 mol fraction of positively charged unit (f^+ = 0.5) prepared in D_2O containing 0.1 M NaCl by the addition of a D_2O solution of $E_{47}M_{106}$ to that of $E_{47}A_{108}$ at C_p = 1.0 g/L. By analogy to the case of a pair of PEG-P(Lys) and PEG-P(Asp) reported by Harada and Kataoka,[6] a stoichiometric mixture (f^+ = 0.5) of $E_{47}M_m$ and $E_{47}A_n$ is expected to form a core−shell micelle. In the polypeptide-based PIC micelle, the PIC of oppositely charged polypeptide blocks

Table 2. Values of Spin−Spin Relaxation Time (T_2) for Protons in PAMPS, PMAPTAC, and PEG Blocks in D_2O Containing 0.1 M NaCl

samples	T_2 at 1.5 ppm (ms)[a]	T_2 at 3.1 ppm (ms)[b]	T_2 at 3.7 ppm (ms)[c]
$E_{47}M_{27}/E_{47}A_{29}$[d]	25	60	407
$E_{47}M_{27}$[e]		262	453
$E_{47}A_{29}$[e]	81		416
$E_{47}M_{106}/E_{47}A_{108}$[d]	2	1	67
$E_{47}M_{106}$[e]		207	476
$E_{47}A_{108}$[e]	54		421

[a] AMPS pendent methyl protons. [b] MAPTAC pendent methyl protons. [c] PEG main chain protons. [d] PIC micelle. [e] Free polymer.

forms a core, and PEG blocks surround the core to form a shell layer. As can be seen in Figure 3c, the intensities of the resonance bands associated with the PMAPTAC and PAMPS blocks are extremely weak compared with those associated with the PEG block. This observation suggests that motions of the PMAPTAC and PAMPS blocks are very restricted as a result of the confinement of these oppositely charged block chains in a PIC micelle core.

To obtain further information about the motional restriction of the PMAPAC and PAMPS blocks when PIC micelles are formed, ^{1}H NMR spin−spin relaxation times (T_2) were measured on $E_{47}M_m$, $E_{47}A_n$, and $E_{47}M_m/E_{47}A_n$ PIC micelles in D_2O containing 0.1 M NaCl. Two matched pairs of the oppositely charged block copolymers, in terms of the lengths of the charged blocks, were chosen to prepare PIC micelles, that is, $E_{47}M_{27}/E_{47}A_{29}$ and $E_{47}M_{106}/E_{47}A_{108}$. Table 2 compares T_2 values for PAMPS pendent methyl protons at 1.5 ppm, PMAPTAC pendent methyl protons at 3.1 ppm, and PEG main chain methylene protons at 3.7 ppm in the PIC micellar state and in the free state. Values of T_2 for free $E_{47}M_{27}$ and $E_{47}A_{29}$ were found to be 262 and 81 ms, respectively, but they became significantly shorter when $E_{47}M_{27}$ and $E_{47}A_{29}$ formed a PIC micelle (i.e., 60 and 25 ms for $E_{47}M_{27}$ and $E_{47}A_{29}$, respectively). This decrease in T_2 is indicative of restricted motions of the charged blocks in the PIC micelle. It should be noted that T_2 values for the longer charged blocks decrease to much smaller values as they form a PIC micelle (i.e., 1 and 2 ms for $E_{47}M_{106}$ and $E_{47}A_{108}$, respectively). This indicates that the motions of the charged blocks are more restricted in the PIC micelle formed from a pair of longer charged blocks.

Static Light Scattering. Apparent values of M_w, R_g, and A_2 for PIC micelles determined by SLS measurements are listed in Table 3. Shown in Figure 4 is a typical example of Zimm plots for $E_{47}M_{106}/E_{47}A_{108}$ PIC micelle. As can be seen from Table 3, the size of the PIC micelle strongly depends on the length of the charged block; the size is larger for longer charged blocks.

The contour length of PMAPTAC and PAMPS blocks with a DP_n of 110 was calculated to be 27.5 nm. Furthermore, the end-to-end distance of a fully extended PEG block with a DP_n of 47 was calculated to be 16 nm.[33,34] The value of $R_g = 55.8$ nm found for the $E_{47}M_{106}/E_{47}A_{108}$ PIC micelle (Table 3) is larger than that expected from the fully extended length of the $E_{47}M_{106}$ and $E_{47}A_{108}$ chains (i.e., ca. 43.5 nm). In fact, it is known that micelles with a PEG outer shell have a tendency to form large aggregates in aqueous solution.[35,36] Thus, a multicore structure formed by the association of individual core−shell micelles may be postulated for the $E_{47}M_{106}/E_{47}A_{108}$ PIC micelle.

The aggregation number (N_{agg}) for the PIC micelle, defined as the total number of polymer chains forming one PIC micelle, can be calculated from the ratio of M_w for the PIC micelle estimated from SLS and M_w for a single polymer chain (unimer) calculated from ^{1}H NMR (M_n) and GPC (M_w/M_n) data. The large N_{agg} for the $E_{47}M_{106}/E_{47}A_{108}$ PIC micelle is indicative of the intermicellar aggregates.

Table 3 also lists results obtained with unmatched pairs, in terms of the block length, of oppositely charged blocks, i.e., $E_{47}M_{27}/E_{47}A_{108}$ and $E_{47}M_{106}/E_{47}A_{29}$ with $f^+ = 0.5$. The molecular weight values for the unmatched pairs of $E_{47}M_{27}/E_{47}A_{108}$ and $E_{47}M_{106}/E_{47}A_{29}$ estimated from SLS (Table 3) are obviously larger than those of unimers (Table 1). Therefore, it is clear that the unmatched pairs exist as a PIC in solution. In a comparison of $E_{47}M_{27}/E_{47}A_{29}$ (matched) and $E_{47}M_{27}/E_{47}A_{108}$ (unmatched) complexes, M_w for the latter is about 6 times larger than that for the former, whereas the aggregation numbers determined as described above are virtually the same ($N_{agg} = 18$). In the case of $E_{47}M_{106}/E_{47}A_{29}$ (unmatched) and $E_{47}M_{106}/E_{47}A_{108}$ (matched) complexes, M_w and N_{agg} for the latter are about 40 and 32 times larger, respectively than those for the former. Thus, it can be concluded that larger PIC micelles are formed from pairs of longer charged blocks. It is inferred from N_{agg} and R_g of the $E_{47}M_{27}/E_{47}A_{108}$ and $E_{47}M_{106}/E_{47}A_{29}$ PIC micelles that the intermicellar aggregation may not occur in the case of the unmatched pairs.

Figure 5 shows the light scattering intensities for matched pairs of $E_{47}M_{106}/E_{47}A_{108}$ and $E_{47}M_{27}/E_{47}A_{29}$ in 0.1 M NaCl as a function of f^+. In this experiment, the total polymer concentration was kept constant at $C_p = 1.0$ g/L. An increase in the scattering intensity indicates an increase in the size (i.e., N_{agg}) for the PIC micelle. A maximum scattering intensity was observed at $f^+ = 0.5$ for both $E_{47}M_{106}/E_{47}A_{108}$ and $E_{47}M_{27}/E_{47}A_{29}$ pairs. These results indicate that stoichiometric charge neutralization in the mixture of the two block copolymers leads to the formation of PIC micelles with maximum aggregation numbers. The same is true for the unmatched pairs of $E_{47}M_{27}/E_{47}A_{108}$ and $E_{47}M_{106}/E_{47}A_{29}$ in 0.1 M NaCl (Figure S1 in the Supporting Information).

Dynamic Light Scattering. Values of the hydrodynamic radius (R_h) for the block copolymers were determined by DLS at $C_p = 1.0$ g/L in 0.1 M NaCl at 20 °C, as listed in Table 1. The R_h values ranging from 4.5 to 6.1 nm appear to be reasonable for unimers of these block copolymers. Figure 6a shows DLS relaxation time (τ) distributions for the $E_{47}M_{106}/E_{47}A_{108}$ and $E_{47}M_{27}/E_{47}A_{29}$ PIC micelles with $f^+ = 0.5$ at $\theta = 90°$. The distributions are unimodal, and the relaxation time at the peak top for the $E_{47}M_{106}/E_{47}A_{108}$ PIC micelle is much longer than that for the $E_{47}M_{27}/E_{47}A_{29}$ PIC micelle. The R_h values for the PIC micelles of $E_{47}M_{106}/E_{47}A_{108}$ and $E_{47}M_{27}/E_{47}A_{29}$ calculated from the relaxation times at the peak top of the relaxation time distribution are 56.9 and 8.3 nm, respectively (Table 3). The R_h value of 8.3 nm for the $E_{47}M_{27}/E_{47}A_{29}$ PIC micelle is smaller than the length value for the fully extended chains of $E_{47}M_{27}$ and $E_{47}A_{29}$ (ca. 23.0 nm), which suggests a simple core−shell structure without intermicellar aggregation. In contrast, the large R_h value of 56.9 nm for the $E_{47}M_{106}/E_{47}A_{108}$ PIC micelle is indicative of the intermicellar aggregation.

The relaxation rates (Γ) measured at different scattering angles are plotted as a function of the square of the magnitude of the scattering vector (q^2) in Figure 6b. A linear relation passing through the origin indicates that all of the relaxation modes are virtually diffusive. These findings suggest that the PIC micelles are spherical in shape.[37] Diffusion coefficients (D) estimated from the slope of the Γ versus q^2 plots were found to be in good agreement with those calculated from Γ at the peak top of the relaxation time distribution obtained at $\theta = 90°$. Because the angular dependence was negligible, R_h values were estimated at a fixed θ of 90°. There was also no angular dependence for the PIC micelles formed from unmatched pairs of $E_{47}M_{27}/E_{47}A_{108}$ and $E_{47}M_{106}/E_{47}A_{29}$ (Figure S2 in the Supporting Information). Table 3 lists R_h values for the PIC micelles estimated at $\theta = 90°$.

Table 3. Dynamic and Static Light Scattering Data for the PIC Micelles in 0.1 M NaCl at 20 °C

samples	R_h (nm)[a]	M_w (SLS) × 10^{-5}[b]	R_g (nm)[b]	A_2 × 10^5 (mol mL/g^2)	R_g/R_h	N_{agg}[c]	dn/dC_p(mL/g)
$E_{47}M_{27}/E_{47}A_{29}$	8.3	1.60	[d]	6.82	[d]	18	0.161
$E_{47}M_{106}/E_{47}A_{108}$	56.9	685	55.8	0.27	0.98	2590	0.157
$E_{47}M_{27}/E_{47}A_{108}$	13.2	9.69	11.6	3.42	0.88	18	0.159
$E_{47}M_{106}/E_{47}A_{29}$	15.7	17.3	15.2	1.39	0.97	80	0.158

[a] Estimated by DLS in 0.1 M NaCl at 20 °C. [b] Estimated by SLS in 0.1 M NaCl at 20 °C. [c] Aggregation number of PIC micelles calculated from M_w of the micelles determined by SLS and M_w of the corresponding unimers determined by GPC. [d] Too small to determine by SLS, i.e., R_g <10 nm.

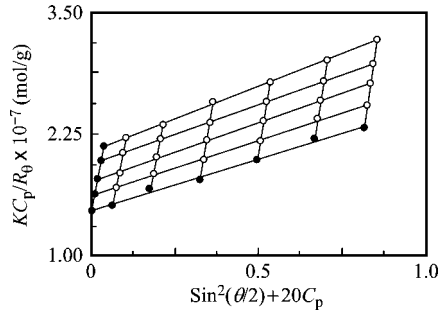

Figure 4. Typical example of Zimm plot for the PIC micelle of $E_{47}M_{106}/E_{47}A_{108}$ with $f^+ = 0.5$ in 0.1 M NaCl aqueous solution at 20 °C at angles from 30 to 130° with a 20° increment. The polymer concentration was varied from 1.0 to 4.0 g/L.

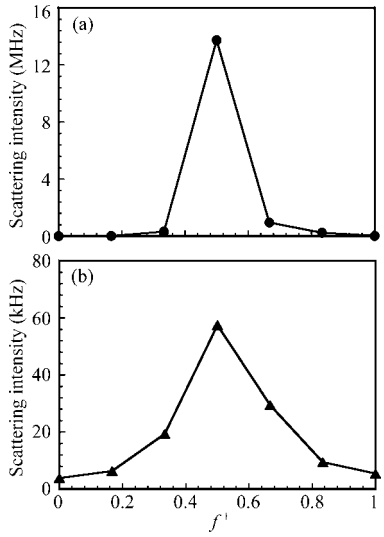

Figure 5. Light scattering intensity of (a) $E_{47}M_{106}/E_{47}A_{108}$ and (b) $E_{47}M_{27}/E_{47}A_{29}$ as a function of f^+ (= [MAPTAC]/([MAPTAC] + [AMPS])) in 0.1 M NaCl aqueous solutions at 20 °C. The concentration of the total block copolymers was fixed at 1.0 g/L.

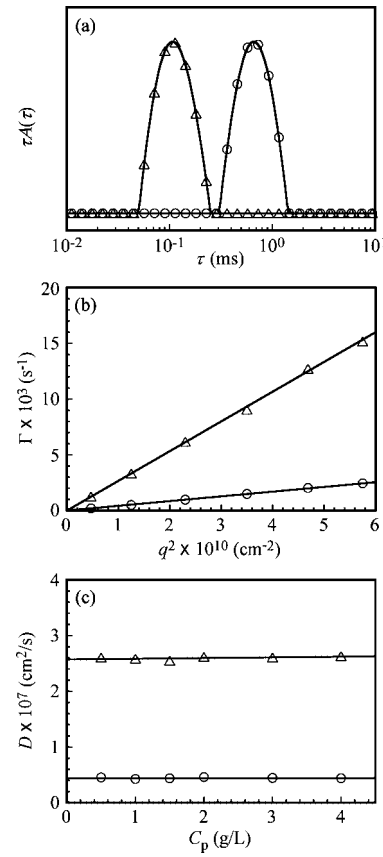

Figure 6. (a) Typical examples of DLS relaxation time (τ) distributions for the PIC micelles of $E_{47}M_{106}/E_{47}A_{108}$ (○) and $E_{47}M_{27}/E_{47}A_{29}$ (Δ) with $f^+ = 0.5$ at $C_p = 1.0$ g/L in 0.1 M NaCl aqueous solutions at 20 °C. (b) Relationship between relaxation rate (Γ) and square of the magnitude of the scattering vector (q^2) for $E_{47}M_{106}/E_{47}A_{108}$ (○) and $E_{47}M_{27}/E_{47}A_{29}$ (Δ) with $f^+ = 0.5$ at $C_p = 1.0$ g/L in 0.1 M NaCl aqueous solutions. (c) Plots of diffusion coefficient (D) for $E_{47}M_{106}/E_{47}A_{108}$ (○) and $E_{47}M_{27}/E_{47}A_{29}$ (Δ) with $f^+ = 0.5$ as a function of C_p in 0.1 M NaCl aqueous solutions.

In Figure 6c, D is plotted against the polymer concentration. Values of D for the PIC micelles are practically constant in the polymer concentration range of $0.5 \le C_p \le 4$ g/L. Because the diffusion coefficients are independent of C_p and the hydrodynamic virial coefficient (k_d) in eq 3 can be negligible, it is suggested that the hydrodynamic size of the PIC micelle is constant independent of C_p. For the unmatched pairs of $E_{47}M_{27}/E_{47}A_{108}$ and $E_{47}M_{106}/E_{47}A_{29}$, the values of D are also independent of C_p (Figure S3 in the Supporting Information).

The ratio of R_g/R_h is useful for characterizing the shape of molecular assemblies. The theoretical value of R_g/R_h for a homogeneous hard sphere is 0.778, and it substantially increases for a less dense structure and a polydisperse mixture; for example, $R_g/R_h = 1.5$ to 1.7 for flexible linear chains in a good solvent, whereas $R_g/R_h \ge 2$ for a rigid rod.[38−40] As listed in Table 3, the R_g/R_h ratio for the PIC micelle of $E_{47}M_{106}/E_{47}A_{108}$ was found to be 0.98. This value suggests that the intermicellar aggregate of the $E_{47}M_{106}/E_{47}A_{108}$ PIC micelles is fairly close to a spherical shape and somewhat polydisperse in size, as suggested by DLS relaxation time distribution data shown in Figure 6a.

Figure 7 shows SEM images for the PIC micelle of $E_{47}M_{106}/E_{47}A_{108}$ with $f^+ = 0.5$. Spheres with a diameter of ca. 100 nm are observed. The size observed by SEM is fairly close to that estimated from light scattering data.

In the case of dynamic micelles formed by small molecular surfactants or by amphiphilic diblock copolymers, unimers coexist with micelles in equilibrium where amphiphiles can undergo exchange between the micelle and bulk phases.[41−43] To clarify whether the PIC micelles in the present study exist in an equilibrium or a kinetically frozen state, we examined whether the block copolymers (unimers) could be exchanged between the PIC micelles of $E_{47}M_{106}/E_{47}A_{108}$ and $E_{47}M_{27}/E_{47}A_{29}$ in water. Figure 7 shows distributions of R_h for the PIC micelles of $E_{47}M_{106}/E_{47}A_{108}$ and $E_{47}M_{27}/E_{47}A_{29}$ along with a 1:1 (w/w) mixture of the two PIC micelles of $E_{47}M_{106}/E_{47}A_{108}$ and $E_{47}M_{27}/E_{47}A_{29}$ at $C_p = 1.0$ g/L in 0.1 M NaCl aqueous solutions. The

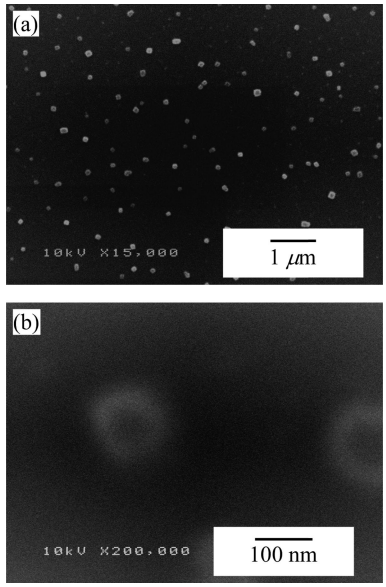

Figure 7. SEM images for the PIC micelle of $E_{47}M_{106}/E_{47}A_{108}$ with $f^+ = 0.5$. The scale bars are (a) 1 μm and (b) 100 nm.

1:1 mixture was prepared by mixing the same volume of 1.0 g/L aqueous solutions of $E_{47}M_{106}/E_{47}A_{108}$ and $E_{47}M_{27}/E_{47}A_{29}$ PIC micelles, and the mixed solution was equilibrated for 1 day at ambient temperature. As can be seen in Figure 8, the size distributions for the PIC micelles of $E_{47}M_{106}/E_{47}A_{108}$ and $E_{47}M_{27}/E_{47}A_{29}$ are well separated and peak at $R_h = 56.9$ and 8.3 nm, respectively. An important observation is that the mixture of the two PIC micelles gives a unimodal size distribution located between the distributions for the $E_{47}M_{106}/E_{47}A_{108}$ and $E_{47}M_{27}/E_{47}A_{29}$ micelles. A value of $R_h = 16.4$ nm was estimated from the distribution peak for the mixture, which is an intermediate value between $R_h = 56.9$ and 8.3 nm for the PIC micelles of $E_{47}M_{106}/E_{47}A_{108}$ and $E_{47}M_{27}/E_{47}A_{29}$. These observations indicate that the exchange of the block copolymers occurs between the PIC micelles within 1 day in aqueous solu tion and yields mixed PIC micelles of the four block copolymers $E_{47}M_{106}$, $E_{47}A_{108}$, $E_{47}M_{27}$, and $E_{47}A_{29}$. Thus, we can conclude that the PIC micelle exists in an equilibrium state and that the PIC micelles formed by matched pairs are not particularly stable compared with those formed by unmatched pairs.

The radius of the core (R_{core}) of the $E_{47}M_{27}/E_{47}A_{29}$ PIC micelle formed at $f^+ = 0.5$ with a simple core−shell structure may be calculated from the volume of each charged block as follows

$$R_{core} = \left(\frac{3V_{core}}{4\pi}\right)^{1/3} = \left(\frac{3}{4\pi N_A}\left(\frac{M_{w,PMAPTAC}}{\rho_{PMAPTAC}} + \frac{M_{w,PAMPS}}{\rho_{PAMPS}}\right)\frac{N_{agg}}{2}\right)^{1/3} \quad (5)$$

where V_{core} is the core volume of a PIC micelle, $M_{w,PMAPTAC}$ and $M_{w,PAMPS}$ are the weight-average molecular weights of the PMAPTAC and PAMPS blocks, respectively, and $\rho_{PMAPTAC}$ and ρ_{PAMPS} are the densities of the PMAPTAC and PAMPS blocks, respectively. From R_h and R_{core}, the shell thickness (L) can be calculated to be $L = R_h - R_{core}$. For the calculation of R_{core}, the bulk densities of MAPTAC and AMPS monomers were used as $\rho_{PMAPTAC} = 1.05$ and $\rho_{PAMPS} = 1.21$ g/cm^3. Thus, values of R_{core} and L for the $E_{47}M_{27}/E_{47}A_{29}$ PIC micelle are calculated to be 3.5 and 4.8 nm, respectively.

The density of the PIC micelle (d_{PIC}) can be calculated by

$$d_{PIC} = \frac{M_{w,PIC}}{(N_A)(V_{PIC})} \quad (6)$$

where $M_{w,PIC}$ is the weight-average molecular weight of a PIC micelle and V_{PIC} is the volume of a PIC micelle. Values of d_{PIC} for the PIC micelles of $E_{47}M_{106}/E_{47}A_{108}$ and $E_{47}M_{27}/E_{47}A_{29}$ are calculated to be 0.142 and 0.111 g/cm^3, respectively. These values are similar to those for the PIC micelles formed from the mixture of PEG-P(Asp) with PEG-P(Lys).[5] The value of d_{PIC} for the intermicellar aggregates of $E_{47}M_{106}/E_{47}A_{108}$ is slightly larger than that for the $E_{47}M_{27}/E_{47}A_{29}$ PIC micelle, which suggests that the intermicellar aggregate is more densely packed than the simple core−shell PIC micelle. The smaller value of d_{PIC} for the $E_{47}M_{27}/E_{47}A_{29}$ PIC micelle implies that the $E_{47}M_{27}/E_{47}A_{29}$ PIC micelle is more hydrated (a greater number of water molecules are present in the micelle) than the $E_{47}M_{106}/E_{47}A_{108}$ PIC micelle.

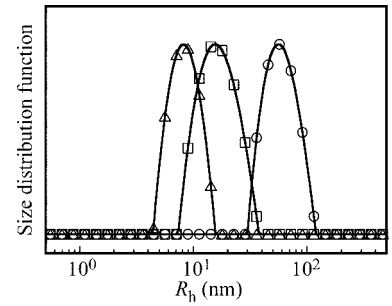

Figure 8. Distributions of R_h for the PIC micelles of $E_{47}M_{106}/E_{47}A_{108}$ (○), $E_{47}M_{27}/E_{47}A_{29}$ (△), and a 1:1 (w/w) mixture of $E_{47}M_{106}/E_{47}A_{108}$ and $E_{47}M_{27}/E_{47}A_{29}$ (□) in 0.1 M NaCl aqueous solutions at 20 °C.

Conclusions

Diblock copolymers, PEG-*b*-PMAPTAC and PEG-*b*-PAMPS, with well-defined block lengths were prepared via RAFT-controlled radical polymerization in water using a PEG-based macro-CTA. Pairs of the oppositely charged block copolymers formed PIC micelles in water. When the MAPTAC/AMPS unit mole ratio was unity, that is, $f^+ = 0.5$, the PIC micelle exhibited a maximum scattering intensity, indicating that the stoichiometric PIC formation is favorable for the micelle formation. Small T_2 values in ^{1}H NMR observed for the core of the PIC micelles suggested that the motions of the core of PIC micelles are very restricted. DLS data suggested that the PIC micelles formed from $E_{47}M_{27}/E_{47}A_{29}$ were spherical in shape with diffusion coefficients remaining unchanged in the concentration range from 0.5 to 4.0 g/L. The N_{agg} and R_h values for the $E_{47}M_{106}/E_{47}A_{108}$ PIC micelles are considerably larger than those for the $E_{47}M_{27}/E_{47}A_{29}$ PIC micelle. Thus, it can be concluded that the oppositely charged diblock copolymers with shorter charged blocks form a simple core−shell PIC micelle whereas those with longer charged blocks form a complicated aggregate. The latter is likely to be an intermicellar aggregate.

Acknowledgment. Financial support by a Grant-in-Aid for Scientific Research (no. 18750105) from the Japan Society for the Promotion of Science (JSPS) is gratefully acknowledged. S.Y. thanks the Iketani Science and Technology Foundation for research funds. We greatly appreciate the assistance of Dr. Takeyuki Kikuchi in obtaining the SEM images.

Supporting Information Available: Light scattering intensities for unmatched pairs of $E_{47}M_{27}/E_{47}A_{108}$ and $E_{47}M_{106}/E_{47}A_{29}$ with varying f^+. Scattering angle and concentration dependence of DLS data for $E_{47}M_{27}/E_{47}A_{108}$ and $E_{47}M_{106}/E_{47}A_{29}$ with $f^+ = 0.5$. This material is available free of charge via the Internet at http://pubs.acs.org.

References and Notes

(1) Chen, S.-C.; Kuo, S.-W.; Liao, C.-S.; Chang, F.-C. *Macromolecules* **2008**, *41*, 8865–8876.

(2) Hurter, P. N.; Hatton, T. A. *Langmuir* **1992**, *8*, 1291–1299.
(3) Kwon, G.; Naito, M.; Yokoyama, M.; Okano, T.; Sakurai, Y.; Kataoka, K. *Langmuir* **1993**, *9*, 945–949.
(4) Vinogradov, S.; Batrakova, E.; Li, S.; Kabanov, A. *Bioconjugate Chem.* **1999**, *10*, 851–860.
(5) Burkhardt, M.; Ruppel, M.; Tea, S.; Drechsler, M.; Schweins, R.; Pergushov, D. V.; Gradzielski, M.; Zezin, A. B.; Muller, A. H. E. *Langmuir* **2008**, *24*, 1769–1777.
(6) Harada, A.; Kataoka, K. *Macromolecules* **1995**, *28*, 5294–5299.
(7) Kakizawa, Y.; Kataoka, K. *Adv. Drug Delivery Rev.* **2002**, *54*, 203–222.
(8) Kataoka, K.; Togawa, H.; Harada, A.; Yagusi, K.; Matsumoto, T.; Katayose, S. *Macromolecules* **1996**, *29*, 8556–8557.
(9) Harada, A.; Kataoka, K. *Macromolecules* **1998**, *31*, 288–294.
(10) Harada, A.; Kataoka, K. *Langmuir* **1999**, *15*, 4208–4212.
(11) Harada, A.; Kataoka, K. *Science* **1999**, *283*, 65–67.
(12) Lokitz, B. S.; Convertine, A. J.; Ezell, R. G.; Heidenreich, A.; Li, Y.; McCormick, C. L. *Macromolecules* **2006**, *39*, 8594–8602.
(13) Li, Y. T.; Lokitz, B. S.; McCormick, C. L. *Angew. Chem., Int. Ed.* **2006**, *45*, 5792–5795.
(14) Xu, X.; Smith, A. E.; Kirkland, S. E.; McCormick, C. L. *Macromolecules* **2008**, *41*, 8429–8435.
(15) McCormick, C. L.; Lowe, A. B. *Acc. Chem. Res.* **2004**, *37*, 312–325.
(16) Lowe, A. B.; McCormick, C. L. *Prog. Polym. Sci.* **2007**, *32*, 283–351.
(17) Mitsukami, Y.; Donovan, M. S.; Lowe, A. B.; McCormick, C. L. *Macromolecules* **2001**, *34*, 2248–2256.
(18) Chong, Y. K.; Le, T. P. T.; Moad, G.; Rizzardo, E.; Thang, S. H. *Macromolecules* **1999**, *32*, 2071–2074.
(19) Meiboom, S.; Gill, D. *Rev. Sci. Instrum.* **1958**, *29*, 688–691.
(20) Mears, S. J.; Cosgrove, T.; Thompson, L.; Howell, I. *Langmuir* **1998**, *14*, 997–1001.
(21) Chu, B. *Laser Light Scattering: Basic Principles and Practice*, 2nd ed.; Academic Press: Boston, 1991.
(22) Jakes, J. *Collect. Czech. Chem. Commun.* **1985**, *60*, 1781–1797.
(23) Brown, W.; Nicolai, T.; Hvidt, S.; Stepanek, P. *Macromolecules* **1990**, *23*, 357–359.
(24) Stockmayer, W. H.; Schmidt, M. *Pure Appl. Chem.* **1982**, *54*, 407–414.
(25) Phillies, G. D. *J. Anal. Chem.* **1990**, *62*, 1049A–1057A.
(26) Phillies, G. D. J. *J. Chem. Phys.* **1988**, *89*, 91–99.
(27) Koppel, D. E. *J. Chem. Phys.* **1972**, *57*, 4814–4820.
(28) Achilleos, M.; Legge, T. M.; Perrier, S.; Patrickios, C. S. *J. Polym. Sci., Part A: Polym. Chem.* **2008**, *46*, 7556–7565.
(29) Boyer, C.; Liu, J.; Wong, L.; Tippett, M.; Bulmus, V.; Davis, T. P. *J. Polym. Sci., Part A: Polym. Chem.* **2008**, *46*, 7207–7224.
(30) Donovan, M. S.; Lowe, A. B.; Sumerlin, B. S.; McCormick, C. L. *Macromolecules* **2002**, *35*, 4123–4132.
(31) Yusa, S.; Fukuda, K.; Yamamoto, T.; Ishihara, K.; Morishima, Y. *Biomacromolecules* **2005**, *6*, 663–670.
(32) Yusa, S.; Konishi, Y.; Mitsukami, Y.; Yamamoto, T.; Morishima, Y. *Polym. J.* **2005**, *37*, 480–488.
(33) Yamamoto, Y.; Nagasaki, Y.; Kato, Y.; Sugiyama, Y.; Kataoka, K. *J. Controlled Release* **2001**, *77*, 27–38.
(34) Tanford, C.; Nozaki, Y.; Rohde, M. F. *J. Phys. Chem.* **1977**, *81*, 1555–1560.
(35) La, S. B.; Okano, T.; Kataoka, K. *J. Pharm. Sci.* **1996**, *85*, 85–90.
(36) Allen, C.; Yu, Y.; Maysinger, D.; Eisenberg, A. *Bioconjugate Chem.* **1998**, *9*, 564–572.
(37) Xu, R.; Winnik, M. A.; Hallett, F. R.; Riess, G.; Croucher, M. D. *Macromolecules* **1991**, *24*, 87–93.
(38) Huber, K.; Bantle, S.; Lutz, P.; Burchard, W. *Macromolecules* **1985**, *18*, 1461–1467.
(39) Akcasu, A. Z.; Han, C. C. *Macromolecules* **1979**, *12*, 276–280.
(40) Konishi, T.; Yoshizaki, T.; Yamakawa, H. *Macromolecules* **1991**, *24*, 5614–5622.
(41) Aniansson, E. A. G.; Wall, S. N. *J. Phys. Chem.* **1974**, *78*, 1024–1030.
(42) Holappa, S.; Kantonen, L.; Winnik, F. M.; Tenhu, H. *Macromolecules* **2004**, *37*, 7008–7018.
(43) Holappa, S.; Kantonen, L.; Andersson, T.; Winnik, F. M.; Tenhu, H. *Langmuir* **2005**, *21*, 11431–11438.

MA8021162